Pol. J. Environ. Stud. Vol. XX, No. X (XXXX), 1-14
DOI: *10.15244/pjoes/220961* ONLINE PUBLICATION DATE: 2026-09-03

Original Research

Hydrochemical Characteristics and Quality Assessment of Limestone Groundwater in the Taiyuan Formation: A Case Study from the Qingdong Coal Mine, China

Xu Liu[1], Jiying Xu[1,3]*, Enping Xue[1], Hongbao Dai[2], Jie Ma[1]

[1]School of Resources and Civil Engineering, Suzhou University, Suzhou, 234000, Anhui, China
[2]School of Environment and Surveying and Mapping Engineering, Suzhou University, Suzhou, 234000, Anhui, China
[3]Coal Industry Engineering Research Center for Exploration and Early Warning of Mine Water Disaster, Anhui University of Science and Technology, 232000, Huainan, Anhui, China

Received: 06 February 2026
Accepted: 21 April 2026

Abstract

This study investigates the hydrochemical characteristics and water quality of limestone water in the Taiyuan Formation at Qingdong Coal Mine, China. A total of 20 water samples were collected and analyzed for major ions. Statistical analysis, Piper and Gibbs diagrams, and ion correlation methods were applied to understand the hydrochemical characteristics and water-rock interactions. Water quality was assessed using single-factor, Nemerow, and fuzzy comprehensive evaluation methods. The results show that the groundwater is slightly alkaline and brackish, dominated by Na^+, Ca^{2+}, SO_4^{2-}, and Cl^-, with the primary hydrochemical type being Ca·Na+K-SO_4·Cl. Water quality assessment indicates that the groundwater is predominantly Class IV and V, with sulfate as the most significant pollutant. These findings provide a scientific basis for the sustainable management of groundwater resources in coal mining regions by elucidating the evaporation-driven hydrochemical evolution of the Taiyuan Formation limestone aquifer.

Keywords: limestone water, Qingdong Coal Mine, hydrochemical characteristics, water quality assessment

Introduction

The chemical composition of coal mine water is essentially the product of long-term interactions between the hydrological cycle system and multiple environmental factors such as climate, hydrology, topography, lithology, and human activities [1]. In recent years, with the accelerated depletion of coal resources and the continuous increase in mining depth, water inrush, recognized as one of the "Five Major Disasters" alongside water hazards, fires, gas, dust, and roof falls, poses a severe threat to safe production [2, 3]. Mine water primarily originates from underground aquifers exposed during excavation. It contains not only

*e-mail: jiyingxu1986@163.com
Tel.: +86-158-0557-4977
0000-0001-6709-3262

high concentrations of suspended solids but may also carry toxic components such as heavy metal ions and acidic pollutants, presenting potential ecological risks to the surrounding environment [4]. Systematically investigating the hydrochemical characteristics and water quality evolution of coal mine water holds dual critical value for both scientific understanding and management practices: it not only enables the precise analysis of groundwater chemical formation mechanisms and the assessment of water resource renewability potential but also supports the development of strategies for the sustainable utilization and protection of groundwater resources [5]. Through targeted treatment processes, mine water can be transformed into a recoverable resource, serving industrial cooling, agricultural irrigation, and domestic water supplementation, thereby achieving synergistic goals of pollution control, resource regeneration, and ecological restoration.

In recent years, China has made significant breakthroughs in hydrochemistry, particularly in the theoretical innovation and technical application of groundwater quality assessment [6]. Research in this domain emphasizes the integration of theoretical exploration with practical application. Currently, a comprehensive methodology system for studying hydrochemical genesis has been established. In practice, preliminary analyses typically employ mathematical statistics and graphical methods, such as Piper trilinear diagrams, to illustrate the spatial distribution and patterns of hydrochemical types. Subsequently, correlation analysis and ion ratio coefficient methods are utilized to identify the sources of dissolved minerals and cation exchange processes. For instance, in the Dongjiang-Hanjiang River Basin, researchers have employed Gibbs models, ion ratio coefficients, factor analysis, water quality index methods, and human health risk assessment models to evaluate groundwater chemistry and quality [7]. Isotopic techniques coupled with hydrogeochemical modeling have become crucial for fine-scale mechanistic studies. These methods enable the quantitative calculation of reaction pathways involving mineral dissolution and precipitation, thereby revealing the evolutionary processes of groundwater chemical composition [8]. Groundwater quality assessment frequently utilizes a range of methods, including single-factor indices, fuzzy comprehensive evaluation, improved grey relational analysis, Nemerow composite indices, and biological integrated assessment [9]. While the single-factor evaluation method remains the foundational tool for official assessments, operating on a “one-vote veto” principle, comprehensive evaluation techniques are being widely applied to more objectively reflect the overall water quality status. These techniques include composite pollution indices, Nemerow indices and their modifications, and entropy-weighted water quality identification indices [10].

Recent international research on hydrochemistry and water quality assessment has been characterized by multidisciplinary intersection, technological integration, and application orientation, achieving significant progress in monitoring network construction, model development, methodological innovation, and cross-domain integration. For instance, innovative approaches such as Principal Component Analysis [11] and multi-indicator comprehensive evaluation systems have emerged in the field of water quality assessment [12]. A comprehensive review of various Water Quality Indices (WQIs) used globally explored their historical development and the challenges in creating an index that can effectively integrate multiple parameters – physical, chemical, and biological – to produce a single score [13]. In the Bundelkhand Massif region of India, identification was conducted using methods such as Piper trilinear diagrams and Durov plots. Analysis of multiple parameters, including Sodium Adsorption Ratio (SAR), Residual Sodium Carbonate (RSC), and Percent Sodium (Na%), indicated that most water samples are unsuitable for irrigation purposes [14]. A multi-indicator assessment of groundwater in the Amaravati River basin has revealed severe water quality issues: nearly 42% of samples fail to meet drinking water standards due to excessive salinity, hardness, nitrate, and fluoride concentrations. Specifically, nitrate health risks were non-compliant in the majority of samples, with non-compliance rates of 81%, 61%, and 39%, respectively, while fluoride hazard indices also remained high at 85%, 68%, and 18% [15]. In contrast, the European Union has established a comprehensive regulatory framework requiring member states to systematically assess the evolution of groundwater quality using standardized statistical analysis methods, such as least squares regression, in accordance with the Water Framework Directive [16].

In the extensive research on mine hydrogeochemistry, the academic community has reached a consensus on several key viewpoints. It is generally accepted that the hydrochemical characteristics of deep aquifers are primarily controlled by water-rock interactions, including the weathering and dissolution of carbonates and silicates, evaporation concentration effects, and cation exchange adsorption. However, despite the wide recognition of these macroscopic mechanisms, limitations remain in existing studies: while research on deep Ordovician limestone water or thin limestone water in North China-type coalfields is abundant, there is still a lack of refined micro-mechanism analysis regarding the hydrochemical evolution path of the Taiyuan Formation thin limestone water intercalated within the coal measures.

This study integrates hydrochemical analysis (Piper diagrams, Gibbs plots, and ion ratio methods) with multiple water quality assessment techniques (single-factor, Nemerow, and fuzzy comprehensive evaluation) to characterize the Taiyuan Formation limestone water in the Qingdong Coal Mine. The findings provide a scientific basis for the sustainable development of groundwater resources in coal mining regions by

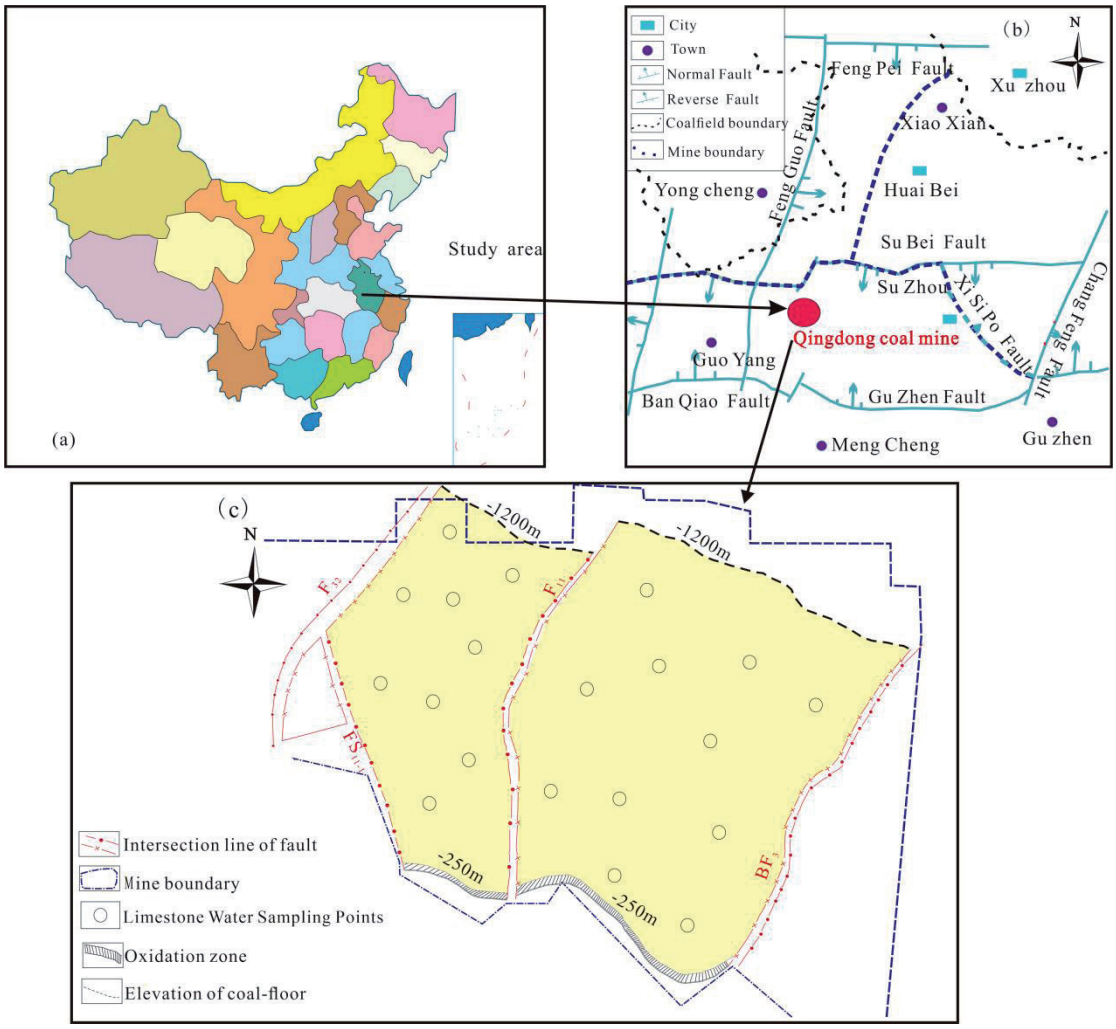

Fig. 1. Geographic location map of the study area and distribution of sampling points.

identifying the evaporation-driven hydrochemical evolution and sulfate pollution sources.

Materials and Methods

Study Area Overview

As illustrated in Fig. 1, the Qingdong Coal Mine, located within the Huaibei Coalfield, is situated in the southwestern part of Suixi County. The mine is bounded by the Haizi and Linhuan coal mines to the east and the F9 fault to the west. Its southern limit is defined by the outcrop line of the top limestone of the Carboniferous Taiyuan Formation; beyond this line, in the Yuandian deep exploration area, lie the Yuandian No. 1 and No. 2 mines. To the north, it extends to the F19 fault and the –1200 m elevation projection line of the 3_2 coal seam, beyond which are the Cuilou and Baishan coal mines across the Qingdong deep prospective area. The topography of the mining area is generally flat, with ground elevations ranging from +27.62 m to +31.37 m, averaging approximately +29 m, and slopes gently from west to east.

A total of 135 boreholes in the area have penetrated the upper section of this formation, revealing a maximum thickness of 60.96 m in Borehole 9-West-4. Lithology is dominated by four layers of gray to dark-gray mudstone bioclastic limestone, interbedded with dark-gray mudstone and thin-bedded fine sandstone. Individual strata generally range from 2 to 3 m in thickness, and the elevated clay content at the top renders this unit a distinct regional marker bed.

Hydrologically, the area is devoid of significant surface water bodies; the primary watercourse is the Jihongxin River, an artificial channel traversing the northwestern sector of the mining area from the southwest to the northeast before eventually discharging into the Bao River. The regional climate is classified as a monsoon-influenced warm-temperate humid subtropical type, characterized by distinct seasonal wind patterns: northeasterly winds prevail during spring and autumn, easterly to southeasterly winds dominate in summer, and northerly to northwesterly winds are typical of winter, with an average wind speed of 3 m/s and maximum

Table 1. Evaluation Indicators

Index	pH	Total hardness	TDS (mg/L)	Chloride (mg/L)	Sulfate (mg/L)
I	6.5≤pH≤8.5	≤150	≤300	≤50	≤50
II		≤300	≤500	≤150	≤150
III		≤450	≤1000	≤250	≤250
IV	5.5≤pH<6.5 8.5<pH≤9.0	≤650	≤2000	≤350	≤350
V	pH<5.5 pH>9.0	>650	>2000	>350	>350

Table 2. Water Quality Classification standards for Nemerow Pollution Index.

Parameter	P	Grade
I	P<1.00	Excellent
II	1.00≤P<2.00	Good
III	2.00≤P<3.00	Better
IV	3.00≤P<4.00	Poor
V	P≧5.00	Very Poor

gusts reaching 18 m/s. Furthermore, the mean annual temperature is 14.6°C, with recorded extremes ranging from a maximum of 41.1°C to a minimum of –21.3°C, and annual precipitation averages 811.8 mm, the majority of which is concentrated during the months of July and August.

In contrast, data from Linhuan Coal Mine in the adjacent area indicate that the formation thickness of this group is 120.30 m, containing 9 to 12 layers of limestone. Six thin coal seams occur between the middle and lower limestone layers, though generally none are of minable value.

Sample Collection, Processing, and Testing

Twenty water samples were collected from dewatering boreholes tapping the limestone aquifer in the underground roadways of the Qingdong Coal Mine. The sampling program included the measurement of physical properties, pH, total hardness, and the concentrations of major ions, specifically Na^++K^+, Ca^{2+}, Mg^{2+}, Fe^{3+}, NH_4^+, Cl^-, SO_4^{2-}, and HCO_3^-. Field measurements of pH and total dissolved solids were conducted in situ using portable instruments. The bicarbonate concentration was determined via acid-base indicator titration. To characterize the hydrochemical properties of the aquifer, statistical analysis and a Piper trilinear diagram were employed. Furthermore, Gibbs plots and ion ratio methods were utilized to identify the controlling factors.

Prior to sampling, the sampling containers were pre-rinsed three times with water from the collection site. At the time of collection, the containers were further flushed three times with the target water sample. Field parameters, including temperature, pH, and total dissolved solids, were recorded in situ. To remove suspended particulates and prevent ion adsorption, all water samples were immediately vacuum-filtered in the field. Filtration was performed using 0.45 μm mixed cellulose ester membrane filters to retain sediments and microorganisms. For samples designated for cation analysis and Total Dissolved Solids, the filtrate was immediately acidified with ultrapure nitric acid to a pH<2 to maintain metal ions in solution during storage. Anion samples were not acidified and were directly sealed in polyethylene bottles. All samples were preserved at 4°C in the dark and transported to the laboratory within 24 h for analysis.

Data Processing and Analysis Methods

Statistical Analysis

The Standards for Groundwater Quality (GB/T 14848-2017) [17] serve as the primary standard for groundwater quality assessment in China. This standard was established by comprehensively considering the current status of groundwater resources, human health benchmarks, and groundwater protection objectives. By referencing the most stringent quality requirements for drinking, industrial, and agricultural water uses, it systematically classifies groundwater into five distinct categories. Detailed classification criteria are summarized in Table 1.

Water quality indicators were selected based on the principles of measurability, comparability, and sensitivity. Given the hydrochemical characteristics of the study area, Total Dissolved Solids, chloride, total hardness, pH, and sulfate were identified as the key influencing parameters.

Single-Factor Index Method

The Single-Factor Index Method [18] is based on environmental quality standards. It assesses groundwater quality by comparing the measured concentrations of individual monitoring parameters against the criteria stipulated in the Standards for Groundwater Quality (GB/T 14848-2017). This method classifies water quality

into five categories: I, II, III, IV, and V. According to the "worst-case scenario dominance" principle, the overall water quality grade is dictated by the parameter with the poorest rating.

1) Calculation Formula When the Evaluation Standard is a Constant

$$G_i = \frac{C_i}{C_0} \tag{1}$$

2) Calculation Formula When the Evaluation Standard is a Range (e.g., pH)

For pH<7.00:

$$G_i = \frac{7.00 - pH}{7.00 - pH_{sd}} \tag{2}$$

For pH>7.00:

$$G_i = \frac{pH - 7.00}{pH_{su} - 7.00} \tag{3}$$

3) Calculation Formula for Water Quality Classification

$$G = MAX(G_i) \tag{4}$$

where C_i denotes the measured concentration of a specific water quality indicator, C_0 denotes the Class III standard limit specified in the Standards for Groundwater Quality (GB/T 14848-2017), G_i denotes the water quality class of the i-th evaluation parameter, pH denotes the measured pH value, pH_{su} denotes the standard's upper limit, and pH_{sl} denotes the standard's lower limit.

Nemerow Pollution Index Method

The Nemerow Pollution Index method constructs a dynamic equilibrium model for environmental quality assessment based on a dual-factor coupling mechanism [19]. It overcomes the systematic limitations of the Single-Factor Index method while maintaining engineering practicality through algorithmic refinement. Characterized by its concise computational procedure and operational convenience, the NPI has become one of the most widely used approaches for evaluating groundwater quality both domestically and internationally.

Expression of the Nemerow Integrated Index:

$$P = \sqrt{\frac{\overline{G_i} + (G_i)^2_{max}}{2}} \tag{5}$$

where P represents the Nemerow Composite Index, Gi represents the mean of the individual indices, and Gimax represents the maximum individual index. Groundwater quality classification is determined based on the value of P according to Table 2.

Fuzzy Comprehensive Evaluation Method

Fuzzy comprehensive evaluation is a methodology rooted in the principles of fuzzy mathematics. By incorporating weights and membership degrees, it transforms multi-factor evaluation problems into quantitative analyses. This approach is particularly well-suited for water quality assessment scenarios characterized by numerous indicators, significant non-linearities, and high levels of uncertainty [20]. The core procedural steps involve constructing the factor and evaluation sets, determining single-factor membership functions, establishing the fuzzy relation matrix, defining the weight matrix, and performing the fuzzy comprehensive evaluation.

Selection of the Factor Set and the Evaluation Set

Taking the Qingdong Coal Mine area as a case study, six indicators – pH, total dissolved solids, Na^+, Cl^-, SO_4^{2-}, and total hardness – were selected to constitute the factor set. The evaluation set was categorized into five grades (Class I, II, III, IV, and V) in accordance with the "Groundwater Quality Standard" (GB/T 14848-2017).

Establishment of Membership Functions

For Class I water (j=1), the membership function is defined as:

$$Z_{ij} = \begin{cases} 1 & x_i \le c_{i1} \\ \dfrac{c_{i_2} - x_i}{c_{i_2} - x_1} & c_{i1} \le x_i \le c_{i2} \\ 0 & x_i \ge c_{i2} \end{cases} \tag{6}$$

For Class II–IV water (j=2, 3, 4), the membership function is defined as:

$$Z_{ij} = \begin{cases} 0 & x_i \ge c_{i(j+1)} \\ \dfrac{x_i - c_{i(j-1)}}{c_{ij} - c_{i(j-1)}} & c_{i(j-1)} \le x_{ij} \le c_{ij} \\ \dfrac{c_{i(j+1)} - x_i}{c_{i(j+1)} - c_{ij}} & c_{ij} \le x_{ij} \le c_{i(j+1)} \end{cases} \tag{7}$$

For Class V water (j=5), the membership function is defined as:

$$Z_{ij} = \begin{cases} 0 & x_i \le c_{i_4} \\ \dfrac{x_i - c_{i_4}}{c_{i_5} - c_{i_4}} & c_{i_4} \le x_i \le c_{i5} \\ 1 & x_i \ge c_{i_5} \end{cases} \tag{8}$$

Table 3. Statistical analysis of Qingdong Coal Mine.

Statistical item	Na^++K^+	Ca^{2+}	Mg^{2+}	Cl^-	SO_4^{2-}	HCO_3^-	TDS	pH
Unit	mg/L							-
Maximum	566.04	553.18	192.99	282.98	2063.76	320.96	3644.73	9.17
Minimum	0.42	0.41	0.35	0.32	0.37	0.12	557.88	7.13
Average	289.73	265.58	107.06	165.57	1151.19	209.61	2601.47	7.93
Standard deviation	180.2	170.6	66.38	102.05	684.97	105.95	777.61	0.43
Coefficient of variation	0.62	0.64	0.62	0.62	0.6	0.51	0.30	0.06

where: x_i is the measured value of the i-th evaluation factor. C_{ij} is the standard value of the j-th grade corresponding to the i-th evaluation factor, and Z_{ij} is the membership degree of the i-th evaluation factor to the j-th grade of water quality. Subsequently, the n×m fuzzy relation matrix B is established based on the membership degrees of the evaluation factors.

Construction of Fuzzy Relation Matrix

Based on the membership degrees of the evaluation factors for the water sample, the n×m fuzzy relation matrix B is established as follows:

$$\begin{pmatrix} z_{11} & z_{12} & \cdots & z_{1m} \\ z_{21} & z_{22} & \cdots & z_{2m} \\ \vdots & \vdots & & \vdots \\ z_{n1} & z_{n2} & \cdots & z_{nm} \end{pmatrix} \quad (9)$$

Construction of the Weight Matrix for Evaluation Factors

Calculation of the weights and the weight matrix. The weight calculation formula is given by:

$$\alpha_i = \frac{x_i/S_i}{\sum_i^n x_i/S_i} \quad (10)$$

where S_i denotes the average value of the evaluation standards for the i-th evaluation factor. Therefore, the 1×n weight matrix A is obtained.

Fuzzy Comprehensive Evaluation

Fuzzy matrix composition operation. By multiplying matrix A and matrix B, matrix D is obtained. The calculation formula is: D=AB. Finally, the fuzzy comprehensive evaluation result is determined based on the principle of maximum membership.

Data Analysis Methods

This study investigates the hydrochemical characteristics of major ions within the aquifer using statistical analysis and Piper trilinear diagrams. Furthermore, Gibbs plots coupled with ionic ratio methods are employed to identify the mechanisms governing the hydrochemistry of limestone water. Descriptive statistics were conducted in Excel. The graphical representations, including Piper diagrams, Gibbs plots, and ionic ratio analyses, were generated using Origin 2025 and subsequently refined and integrated using CorelDRAW 2024.

Results and Discussion

Hydrochemical Characteristics

A statistical analysis was performed on the major ions, pH, and TDS values of the limestone water samples collected from the study area, with the results summarized in Table 3.

Table 3 presents the statistical characteristics of the hydrochemical parameters of the Taiyuan Formation limestone water in the Qingdong Coal Mine. The pH values range from 7.13 to 9.17, with a mean of 7.93, indicating slightly alkaline water. The TDS values vary from 557.88 to 3644.73 mg/L, suggesting poor water quality characterized as brackish water [15]. The mean concentrations of cations follow the order: Na^+>Ca^{2+}>Mg^{2+} (289.73, 265.58, and 107.06 mg/L, respectively), while the anions follow the order: SO_4^{2-}>Cl^->HCO_3^- (1151.19, 2601.47, and 209.61 mg/L, respectively). Consequently, Na^+, Ca^{2+}, SO_4^{2-}, and Cl^- are identified as the dominant ions in the study area. Furthermore, the low coefficients of variation (all<1) for all ions suggest a relatively stable hydrochemical environment with minimal external influence [21]. Based on the hydrochemical analysis, the limestone water in the study area is classified as a Na+K·Ca-SO_4·Cl type. The high concentration of SO_4^{2-} likely originates from gypsum dissolution and sulfide mineral oxidation, whereas the enrichment of Na^+ is closely

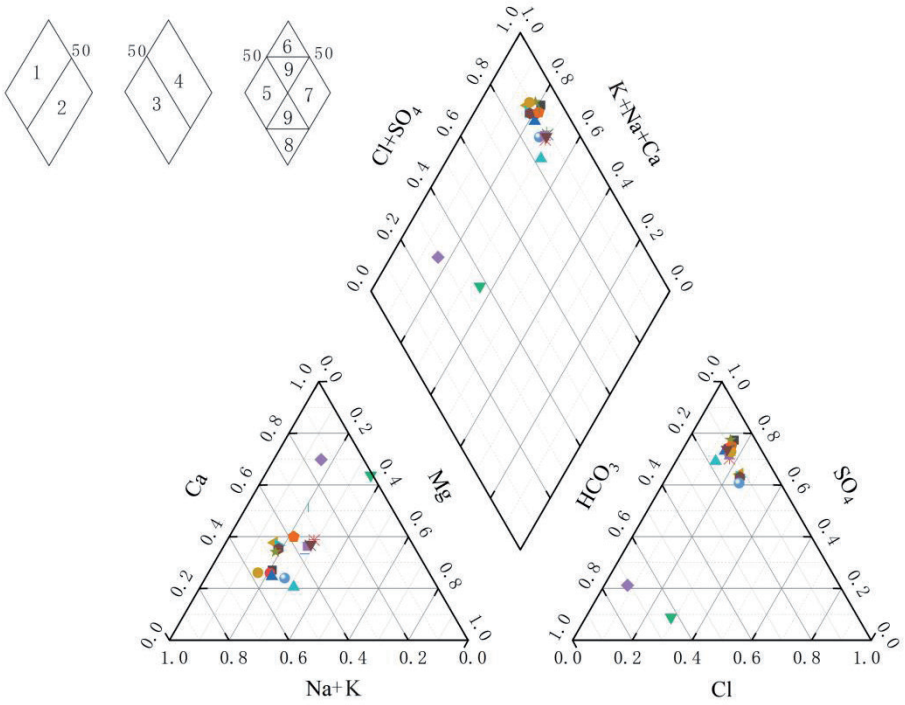

Fig. 2. Piper diagram of sandstone fissure water samples.

related to silicate weathering and cation exchange adsorption. Spatially, the TDS values in the northwest are significantly higher than those in the southeast, which may be attributed to differences in aquifer runoff conditions and resultant leaching intensity. The stable hydrochemical environment (coefficient of variation, 0.06<CV<0.62) reveals a relatively closed hydrodynamic system where water-rock interactions dominate the ionic composition. The hydrochemical signature of this area is developed within a relatively closed hydrodynamic system, resulting from the combined effects of multiple geochemical reactions, including gypsum dissolution, sulfide oxidation, silicate weathering, and cation exchange. In particular, the high salinity zone in the northwest reflects the cumulative effects of long-term water-rock interactions. These findings hold critical implications for assessing mine water inrush sources and predicting water quality evolution.

Water-Rock Interaction

The Piper diagram, a fundamental tool in hydrogeochemical analysis, illustrates the relative proportions of major ions in groundwater and characterizes its general chemical features, enabling the investigation of hydrochemical evolution patterns. Divided into nine distinct zones, the diamond-shaped Piper diagram allows for the classification of water samples based on their unique chemical signatures. As shown in Fig. 2, the Taiyuan Formation limestone water samples predominantly fall within Zone 1 for cations and Zone 4 for anions, with the majority clustering in Zone 6 of the central diamond. Cation distribution reveals that Ca^{2+} and Na^{+}+K^{+} are the dominant ions, with alkali metals exceeding alkaline earth metals in Zone 1. Anion analysis shows SO_4^{2-} as the predominant species, accounting for 62%-85% of total anions and clearly dominating Zone 4, where strong acid anions outweigh weak acid anions. The concentration of samples in Zone 6, characterized by non-carbonate hardness exceeding 70%, confirms the prevalence of sulfate-chloride type water with a Ca·Na+K-SO_4·Cl chemical classification. The hydrochemical characteristics suggest that the enrichment of Na^{+} and K^{+} in Zone 1 likely originates from evaporite dissolution or silicate weathering processes. The overwhelming dominance of SO_4^{2-} in Zone 4 indicates significant contributions from gypsum dissolution and sulfide mineral oxidation. The stable near-neutral pH conditions, combined with the high non-carbonate hardness, reflect a hydrogeochemical system controlled by sulfate-chloride leaching processes under semi-confined hydrogeological conditions. The Ca·Na+K-SO_4·Cl hydrochemical facies of the Taiyuan Formation limestone water represents a comprehensive manifestation of multiple coupled geochemical processes, including evaporite dissolution, sulfide oxidation, and potential cation exchange, acting synergistically over a prolonged period within a deep, semi-confined, and stagnant aquifer environment.

The Gibbs diagram serves as a diagnostic tool to identify the principal mechanisms governing hydrochemical evolution and to elucidate the relationship between water chemistry and climatic or lithological characteristics [22]. By analyzing major ion concentrations in global water bodies, including rivers, lakes, and seawater, Gibbs established plots of

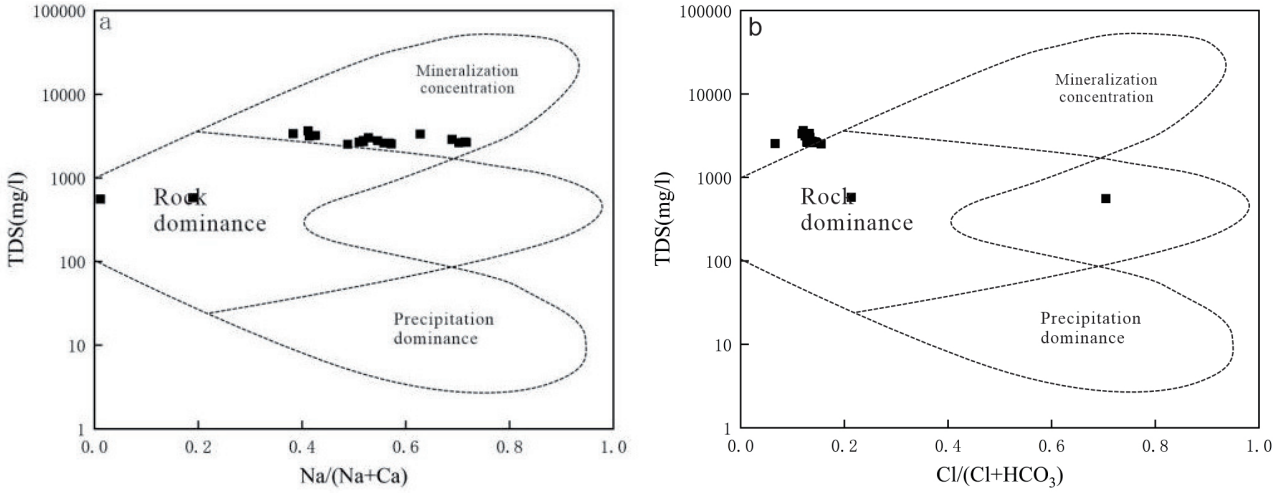

Fig. 3. Gibbs diagram of limestone water.

TDS versus $Na^+/(Na^+ + Ca^{2+})$ and $Cl^-/(Cl^- + HCO_3^-)$. These plots demarcate the natural factors controlling solute sources into three distinct domains: mineralization concentration, atmospheric precipitation, and rock weathering [23]. This method facilitates a visual interpretation of the dominant controlling factors. As illustrated in Fig. 3, the Gibbs plots for the Taiyuan Formation limestone water reveal TDS values ranging from 557.88 to 3644.73 mg/L. The $Na^+/(Na^+ + Ca^{2+})$ molar ratios vary between 0.01 and 0.72, while the $Cl^-/(Cl^- + HCO_3^-)$ ratios range from 0.06 to 0.54. Notably, all data points are clustered in the upper section of both diagrams, falling squarely within the mineralization concentration field. This distribution suggests that evaporation is the primary process influencing the hydrochemical composition of the limestone water [24]. A significant positive correlation is observed between TDS and both the cation ratio $(Na^+/(Na^+ + Ca^{2+}))$ and the anion ratio $(Cl^-/(Cl^- + HCO_3^-))$, with samples concentrated in the upper-right quadrant indicative of mineralization concentration. The 6.5-fold variation in TDS values indicates varying degrees of mineralization concentration of dissolved salts. Furthermore, the high proportions of Na^+ (up to 72%) and Cl^- (up to 54%) imply the preferential enrichment of highly soluble salts, such as halite, under the prevailing evaporation regime. This hydrochemical signature is likely attributable to intense evapotranspiration driven by the local semi-arid climate. Concurrently, the stagnant groundwater flow within the limestone fracture systems provides favorable hydrogeological conditions for the accumulation of dissolved salts.

Ion Source Analysis

The Pearson correlation coefficient is a statistical metric used to quantify the strength and direction of the linear relationship between two continuous variables [25]. With values ranging from –1 to +1, r = 1 indicates a perfect positive correlation, r = –1 a perfect negative correlation, and r = 0 the absence of a linear relationship.

In hydrogeochemical studies, a significant positive correlation between ions typically indicates a common source, such as the synergistic dissolution of the same rock-forming mineral. Conversely, a negative correlation often reflects competitive geochemical mechanisms, such as cation exchange or mineral precipitation. Consequently, correlation analysis provides a critical statistical basis for quantitatively interpreting the origins and evolutionary pathways of groundwater chemical components.

Fig. 4 presents the results of the correlation analysis for major ions in the groundwater of the study area, based on the Pearson correlation coefficient method.

As shown in Fig. 4, TDS exhibits a highly significant positive correlation with Cl^- and SO_4^{2-}, while a strong positive correlation is also observed between SO_4^{2-} and Cl^-. Furthermore, the correlation coefficients between $Na^+ + K^+$, Ca^{2+}, and Mg^{2+} with TDS are 0.78, 0.77, and 0.71, respectively, indicating strong positive correlations. These results suggest that the groundwater salinity in the study area is primarily controlled by Cl^- and SO_4^{2-}. The high correlation between SO_4^{2-} and Cl^- implies a common origin or control mechanism, most likely intense evaporation and concentration, which leads to the synchronous enrichment of salts in the groundwater.

Positive correlations are generally observed among the ions, particularly between Ca^{2+} and Mg^{2+}, as well as between Mg^{2+} and $Na^+ + K^+$. The significant positive correlation between Ca^{2+} and Mg^{2+} typically indicates a common origin, most likely attributed to the dissolution of dolomite $[CaMg(CO_3)_2]$ in the aquifer. Meanwhile, the positive correlations of $Na^+ + K^+$ with Ca^{2+} and Mg^{2+}, combined with the aforementioned dominance of evaporation and concentration, suggest that the dissolution of halite and sulfate minerals constitutes the primary source of these ions in this environment.

The pH value exhibits generally weak correlations with other chemical parameters. For instance, the

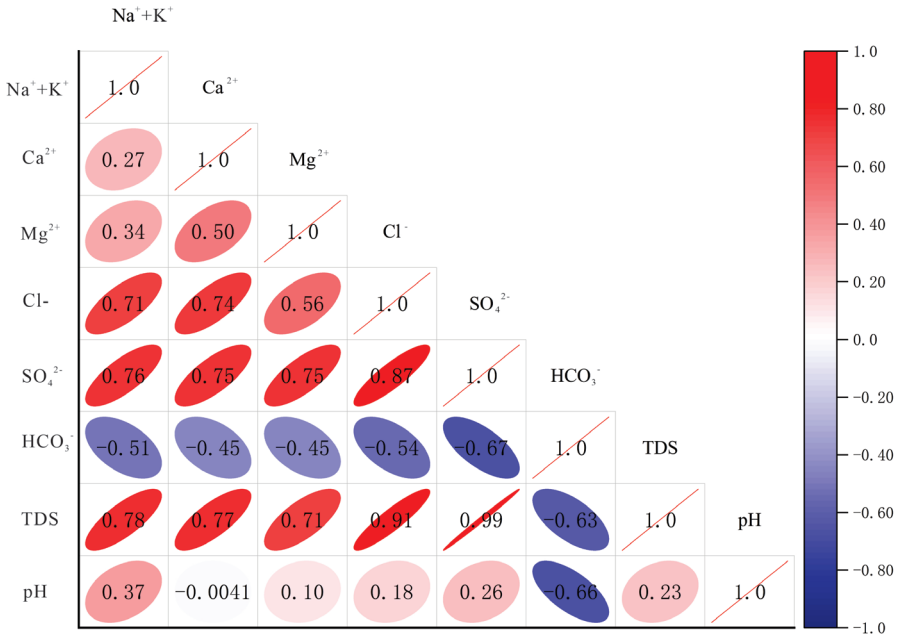

Fig. 4. Pearson correlation matrix of major ions.

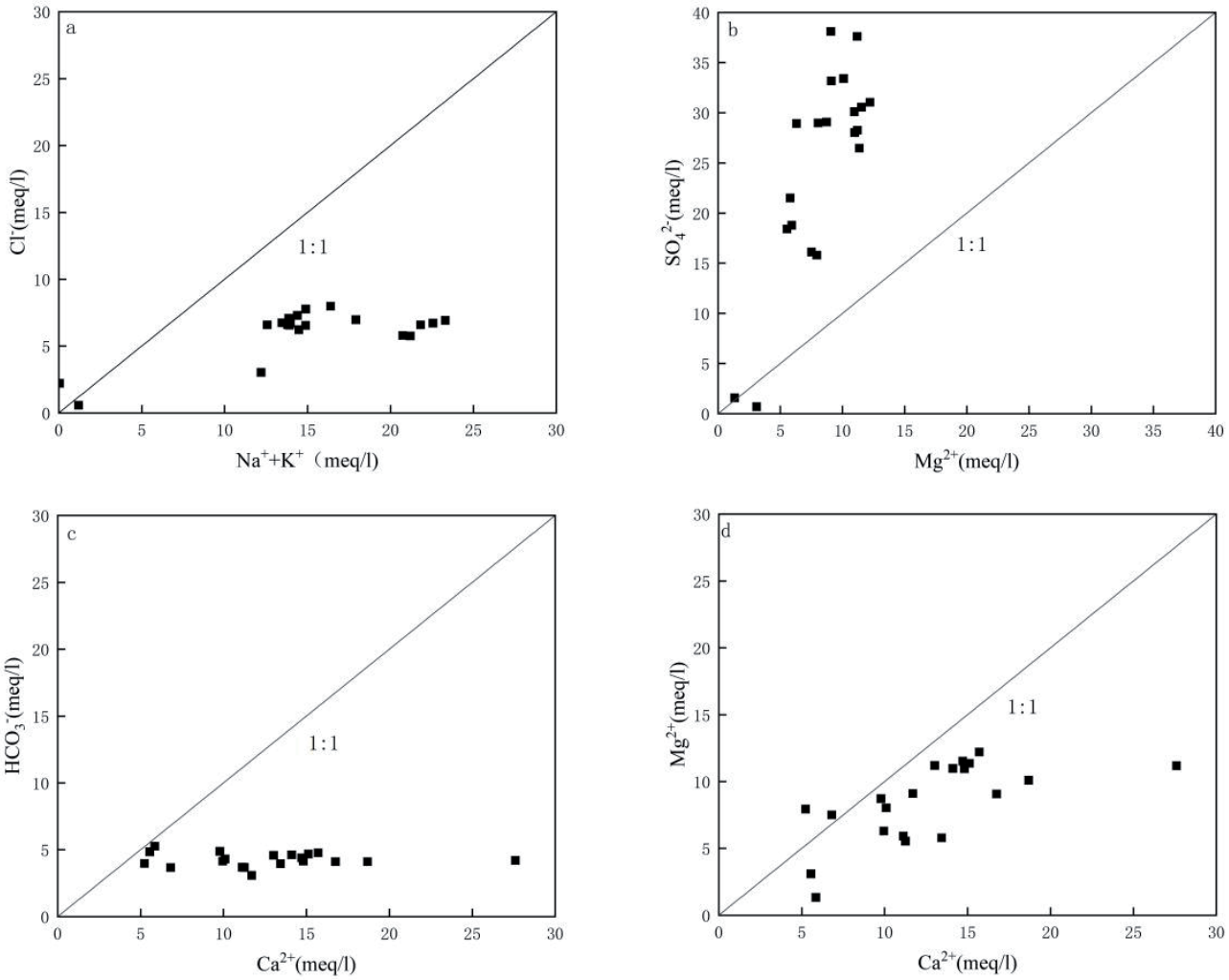

Fig. 5. Ion analysis diagram of limestone water.

correlation coefficient between pH and HCO_3^- is only −0.66, and that with TDS is merely 0.23, while pH shows almost no correlation with Ca^{2+}. This indicates that the groundwater pH in the study area is primarily governed by its intrinsic acid-base buffering system and is less affected by evaporation concentration or salt accumulation.

Ion Ratio Analysis

Ion ratio analysis is employed to investigate the chemical composition and concentration characteristics of groundwater. By examining the molar or mass ratios between various hydrochemical parameters, specific hydrogeochemical processes can be elucidated [26]. The ion ratio plots for the Taiyuan Formation limestone water are presented in Fig. 5.

The Na^+/Cl^- ratio serves as a crucial indicator for tracing the source of sodium in groundwater, helping to distinguish between halite dissolution, silicate weathering, and cation exchange processes. In Fig. 5a), although the data points generally cluster around the 1:1 stoichiometric line, suggesting a primary influence from halite dissolution, most samples plot slightly below it. This deviation indicates that Na^+ is derived from sources other than halite alone. Specifically, the lower Na^+/Cl^- ratios suggest either the dissolution of sodium-bearing silicate minerals or, more significantly, active cation exchange within the aquifer. During cation exchange, Na^+ is preferentially desorbed into the aqueous phase, while Ca^{2+} or Mg^{2+} ions are adsorbed onto mineral surfaces. This base-exchange process typically results in a relative enrichment of Na^+ compared to Cl^-. Additionally, localized evaporation may concentrate both ions; however, given the high solubility and conservative nature of Cl^-, the observed Na^+ enrichment is predominantly attributed to water-rock interactions and ion exchange rather than evaporative effects.

The molar ratio of Mg^{2+} to SO_4^{2-} provides insights into the dissolution of sulfate minerals, potential anthropogenic contamination, specific hydrogeological settings, or natural mineralization processes [26]. As shown in Fig. 5b), the Mg^{2+}-SO_4^{2-} ion plot indicates that these ions in the coal-measure water are primarily derived from sulfate mineral dissolution. However, the data points plot predominantly above the 1:1 reference line, suggesting that the concentration of SO_4^{2-} significantly exceeds that of Mg^{2+}. This deviation implies the presence of sulfide minerals within the limestone strata. As groundwater migrates through sulfate-rich geological layers, the oxidation of these sulfide minerals generates sulfuric acid, leading to enhanced dissolution of sulfate minerals and a consequent increase in SO_4^{2-} concentration. Furthermore, prolonged flow paths and extended residence times facilitate extensive water-rock interactions, allowing for greater dissolution of minerals and the accumulation of solutes. Other ratios fall below the 1:1 line. The high concentration of Ca^{2+} in the water suggests that SO_4^{2-} may combine with Ca^{2+} to form a gypsum precipitate. This leads to a decrease in SO_4^{2-} concentration, while Mg^{2+} does not participate in the precipitation, resulting in a relative depletion of SO_4^{2-}.

Ca^{2+} and HCO_3^- are the predominant ions in limestone water. The stoichiometric plot of Ca^{2+} versus HCO_3^- is shown in Fig. 5c). Although the dissolution of calcite, the primary constituent of limestone, typically produces equimolar amounts of Ca^{2+} and HCO_3^-, the molar ratio of Ca^{2+}/HCO_3^- in the samples is generally greater than 1 [27]. This indicates that Ca^{2+} originates not only from carbonate dissolution but also from the weathering of other calcium-bearing minerals, such as silicates or gypsum, without a corresponding increase in HCO_3^- concentration. Furthermore, it is geochemically characteristic that calcium concentrations in limestone aquifers typically exceed magnesium concentrations, reflecting the relative abundance of calcite compared to dolomite in the formation.

Fig. 5d) presents the molar plot of Mg^{2+} versus Ca^{2+}. The data points predominantly plot below the 1:1 reference line, indicating that the concentration of Ca^{2+} significantly exceeds that of Mg^{2+} [28]. This geochemical signature is consistent with the petrological characteristics of the limestone formation. Limestone is primarily composed of calcite, a mineral structurally dominated by calcium with low magnesium content [29]. Consequently, when limestone interacts with groundwater, the preferential dissolution of calcite results in the release of Ca^{2+} into the aqueous phase, leading to higher Ca^{2+} concentrations relative to Mg^{2+}.

Water Quality Assessment

Evaluation Results

The results obtained using the single-factor evaluation method, the Nemerow index method, and the fuzzy comprehensive evaluation method are presented in Tables 4, 5, and 6, respectively.

As shown in Table 4 and Fig. 6, twenty samples were evaluated for each parameter. All 20 samples for pH fall within Class I, indicating minimal pollution. In stark contrast, the total hardness results reveal severe degradation: only 5 samples meet Class I standards, while the remaining 15 are classified as Class V, yielding a compliance rate of merely 25%. Similarly, the TDS levels are predominantly poor, with 17 out of 20 samples categorized as Class IV, alongside 2 Class I samples and 1 Class V sample. Regarding specific ionic composition, chloride concentrations vary from Class I to Class IV, though the majority fall within Class III. Sulfate pollution is particularly severe; with the exception of one sample in Class I and one in Class II, all others are classified as Class V. In summary, although pH complies with the standard, total hardness and sulfate exhibit severe exceedances. Furthermore, TDS and chloride show widespread contamination, rendering the groundwater unsuitable for drinking by the local population.

Table 4. Evaluation results of Groundwater Quality (Single-Factor Evaluation Method).

Sample	pH		Total hardness		TDS		Chloride		Sulfate	
	G_i	Type	G_i	Type	G_i	Type	G_i	Type	G_i	Type
1	1.00	I	0.13	I	2.88	IV	0.95	III	6.38	V
2	0.47	I	0.11	I	2.64	IV	0.82	III	5.57	V
3	0.43	I	0.12	I	2.69	IV	0.82	III	5.59	V
4	0.40	I	0.05	I	0.56	I	0.31	II	0.13	I
5	0.27	I	0.04	I	0.58	I	0.08	I	0.30	II
6	0.16	I	4.28	V	3.64	V	1.13	IV	8.26	V
7	0.55	I	3.74	V	3.15	IV	1.00	IV	7.07	V
8	0.60	I	3.79	V	3.21	IV	1.03	IV	7.21	V
9	0.59	I	2.87	V	3.34	IV	0.98	III	7.32	V
10	0.43	I	3.20	V	3.02	IV	0.99	III	6.42	V
11	0.73	I	3.12	V	2.79	IV	0.92	III	6.19	V
12	0.64	I	2.87	V	2.68	IV	0.96	III	5.78	V
13	0.29	I	2.92	V	2.72	IV	0.93	III	5.87	V
14	0.09	I	2.94	V	2.52	IV	0.93	III	5.09	V
15	0.21	I	2.69	V	2.61	IV	0.93	III	5.43	V
16	0.53	I	4.31	V	3.37	IV	1.10	IV	7.23	V
17	0.22	I	2.69	V	2.61	IV	0.89	III	5.44	V
18	0.53	I	1.81	V	2.66	IV	0.93	III	5.56	V
19	0.47	I	2.93	V	2.55	IV	0.43	II	6.07	V
20	0.53	I	3.10	V	2.80	IV	0.88	III	5.96	V
Average	0.457		2.39		2.65		0.85		5.64	
Maximum	1		4.31		3.64		1.13		8.26	

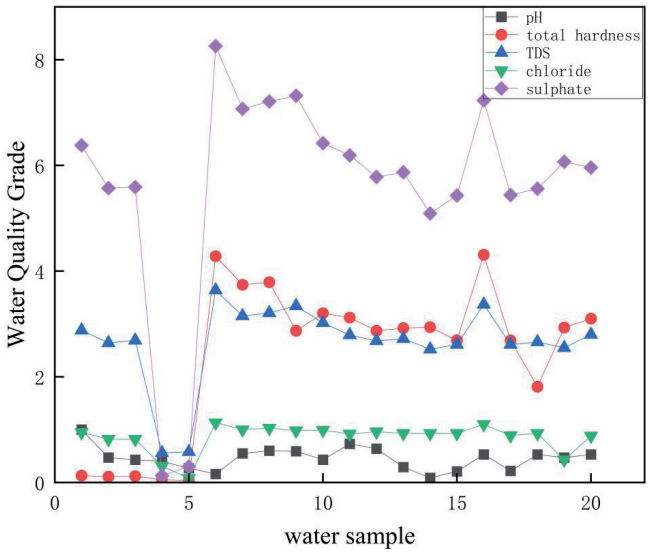

Fig. 6. Evaluation results of Groundwater Quality (Single-Factor Evaluation Method).

Table 5. Evaluation results of Groundwater Quality (Nemerow Index Method).

Sample	pH	Total hardness	TDS	Chloride	Sulfate
Nemerow Composite Index	0.78	3.49	3.18	1	7.07
Type	I	IV	IV	II	V

Table 6. Fuzzy comprehensive evaluation results.

Fuzzy comprehensive evaluation results						
Number	I	II	III	IV	V	Grade
1	0.01	0.005	0.04	0.05	0.92	V
2	0.0128	0.0062	0.1262	0.0598	0.5203	V
3	0.0127	0.0063	0.1281	0.0549	0.5285	V
4	0.2384	0.2751	0.4865	0.0000	0.0000	III
5	0.2237	0.7461	0.0302	0.0000	0.0000	II
6	0.0340	0.0120	0.0211	0.1181	0.7951	V
7	0.0000	0.0000	0.0387	0.1165	0.7979	V
8	0.0000	0.0000	0.0392	0.1115	0.8058	V
9	0.0000	0.0000	0.0378	0.0832	0.7549	V
10	0.0000	0.0000	0.0522	0.0759	0.7082	V
11	0.0000	0.0000	0.0399	0.1311	0.7632	V
12	0.0000	0.0000	0.0455	0.1406	0.7389	V
13	0.0000	0.0038	0.0719	0.1004	0.7517	V
14	0.0410	0.0241	0.0124	0.1152	0.7243	V
15	0.0535	0.0125	0.0135	0.0930	0.7482	V
16	0.0000	0.0000	0.0531	0.0878	0.8248	V
17	0.0556	0.0114	0.0202	0.0838	0.7499	V
18	0.0000	0.0000	0.0648	0.0882	0.6415	V
19	0.0000	0.0144	0.0756	0.0671	0.7625	V
20	0.0000	0.0000	0.0645	0.0962	0.7724	V

The calculated Nemerow index values are shown in Table 5: pH 0.78, total hardness 3.49, total dissolved solids 3.18, chloride 1.00, and sulfate 7.07. Corresponding groundwater quality classifications are excellent, poor, poor, good, and very poor, respectively.

As shown in Table 6, the evaluation results indicate that 16 sampling sites are classified as Class V water, with only a few sites meeting the standards for Class III or Class II. The overall water quality status of the study area is concerning; the majority of the water bodies fall into the inferior Class V category, indicating that the water quality is predominantly poor.

Comparative Analysis

The three methods yield distinct evaluation results due to their differing theoretical orientations. The single-factor method adheres to a "one-vote veto" principle, determining the overall water quality grade solely based on the single most polluted indicator [29]. In contrast, the Nemerow index method employs a mathematical weighting model that incorporates both peak pollution levels and average values; this approach highlights the risks posed by high-concentration pollutants while accounting for the overall pollution status [30]. The fuzzy comprehensive evaluation method is particularly suitable for scenarios characterized by numerous indicators, significant non-linearity, and high uncertainty [31]. Conceptually, the single-factor method "amplifies the weakest link", whereas the Nemerow method "balances the global perspective", and the fuzzy method addresses complexity; combining the three allows for a balance between risk control and systematic management. A comparison of the three methods reveals consistent

results for pH and chloride, indicating good water quality. However, discrepancies arise regarding total hardness, total dissolved solids, and sulfate. While the single-factor method focuses on individual exceedances, the Nemerow index method comprehensively considers the influence of multiple indicators. Consequently, for parameters with severe exceedances like total hardness and sulfate, the Nemerow method assigns a lower water quality category, better reflecting the integrated pollution status. The fuzzy comprehensive evaluation classifies the overall water quality as Class V. These results collectively indicate that the Taiyuan Formation limestone water in the Qingdong Coal Mine is of poor quality [32].

Conclusions

Based on data collected from the Taiyuan Formation limestone water in Qingdong Coal Mine, hydrochemical characteristics were analyzed using statistical analysis, the Piper diagram, Gibbs plots, and ion correlation diagrams. The following conclusions and recommendations were drawn:

(1) Groundwater in the study area is slightly alkaline brackish water, with a dominant hydrochemical facies of Ca·Na+K-SO_4·Cl. Comprehensive assessments consistently classify the water quality as predominantly Class IV and V. Sulfate is identified as the primary pollutant, exceeding regulatory standards in the majority of samples. This contamination poses a direct threat to safe mining operations and renders the water unsuitable for drinking or agricultural purposes.

(2) Ion ratio analysis suggests that Mg^{2+} and SO_4^{2-} in the coal-measure water samples are primarily derived from sulfate dissolution, while Na^+ and Cl^- originate from the dissolution of sodium salts and halite, along with the influence of evaporation and concentration. Ca^{2+} is mainly sourced from the dissolution of carbonates and other calcium-bearing minerals.

(3) Targeted control of sulfate pollution is urgently needed given the pervasive sulfate enrichment (majority of samples exceeding Class V), which requires a multi-pronged strategy including grouting to seal gypsum dissolution pathways, real-time sulfate monitoring with tiered water management, and the application of sulfate-resistant materials for corrosion protection.

(4) This study provides a critical scientific foundation for the sustainable development of groundwater resources by identifying the evaporation-driven mechanisms and sulfate pollution sources in the Taiyuan Formation limestone aquifer, thereby informing targeted water management and protection strategies.

Acknowledgements

This research was supported by the Anhui Provincial College Students' Innovation and Entrepreneurship Training Project (Grant No. S202510379070) and the Open Fund of the Coal Industry Engineering Research Center for Exploration and Early Warning of Mine Water Disaster (Grant No. 2024-CIERC-07). The authors also acknowledge financial support from the Excellent Young Teachers Training Program of Anhui Province (Grant No. YQYB2024075), the Academic and Technical Leader Reserve Program of Suzhou University (Grant No. 2024XJHB08), the Postdoctoral Research Startup Fund Project of Suzhou University (2025BSH001), and the Drilling Engineering Technology Research Center of Suzhou University (2024PT04). Additional financial support was provided by the Anhui Provincial Department of Education Research Project (2023AH052224), the Anhui Provincial Department of Education Quality Engineering Projects (2024zygzts115; 2024jsqygz117), the Suzhou University Institutional Quality Engineering Project (szxy2023xxhz01), and the National Innovation and Entrepreneurship Training Program for College Students (202510379057), which provided important assistance for the completion of this study.

AI Usage Disclosure Statement

During the preparation of this manuscript, the authors used DeepSeek (web version, V3) for language polishing, grammar checking, and expression refinement. After using this tool, the authors carefully reviewed and edited the content as needed and take full responsibility for the final version of the manuscript.

Conflict of Interest

The authors declare no conflict of interest.

References

1. NIU C., TIAN Q., XIAO L., XUE X., ZHANG R., XU D., LUO S. Principal causes of water damage in mining roofs under giant thick topsoil-lilou coal mine. Applied Water Science, **14** (6), 1, **2024**.
2. WU M., YE Y., HU N., WANG Q., TAN W. Visualization Analysis and Progress of Mine Water Inrush Disaster-Related Research. Mine Water and the Environment, **41**, 599, **2022**.
3. LU C., CHENG W., YIN H., ZHANG S., CHENG Y., DONG F., ZHANG X., ZHANG X. Study on inverse geochemical modeling of hydrochemical characteristics and genesis of groundwater system in coal mine area-a case study of Longwanggou Coal Mine in Ordos Basin. Environmental Science and Pollution Research, **31**, 16583, **2024**.
4. LI X., CAI J., CHEN D., FENG Q. Characteristics of water contamination in abandoned coal mines: a case study on Yudong River area, Kaili, Guizhou Province, China. International Journal of Coal Science Technology, **8**, 1491, **2021**.
5. MA M., YU Y., YAN B., TUO Y., GAI J. Hydrochemical

Evolution and Formation Mechanism of Groundwater Affected by Human Activities in Zhangxuan Basin, Northwest of Yanshan Mountains, China. PLoS One, **20** (2), e0318995, **2025**.
6. PARETA K., PAREA U. Hydrogeochemical Analysis of Groundwater of a Microwatershed (MWS) of Banas River Basin, Rajasthan, India. International Journal of Environmental Chemistry, **9** (1), 1, **2023**.
7. LU L., WANG Z., WANG Z., DENG L., ZOU S., FAN L., YANG Y. Chemical Characteristics and Water Quality Assessment of Groundwater in the Dongjiang-Hanjiang River Basin, China. Journal of Environmental Chemical Engineering, **12** (6), 114721, **2024**.
8. CHEN J., WANG Y., SU A. Composition characteristics of magnesium isotopes in groundwater and their application prospects in water cycle processes. Environmental Earth Sciences, **83**, 407, **2024**.
9. ZHANG H., SUN H., BIAN K., NIU Y., YANG H., YANG J., PANCHAL B. Seasonal Variation Characteristics of Karst Groundwater Chemistry and Water Quality Assessment in the Northern Part of the Baiquan Spring Area. Journal of Water Chemistry and Technology, **46** (1), 80, **2024**.
10. YANG Y., LI P., ELUMALAI V., NING J., XU F., MU D. Groundwater Quality Assessment Using EWQI With Updated Water Quality Classification Criteria: A Case Study in and Around Zhouzhi County, Guanzhong Basin (China). Exposure and Health, **15**, 825, **2023**.
11. DHEERAJ V.P., SINGH C.S., SONKAR A.K., KISHORE N. Heavy Metal Pollution Indices Estimation and Principal Component Analysis to Evaluate the Groundwater Quality for Drinking Purposes in Coalfield Region, India. Sustainable Water Resources Management, **10**, 31, **2024**.
12. WANG B., CHEN Q., YUN M.H., HUANG J.J., SUN J.M. Development of a comprehensive pollution evaluation system based on entropy weight-fuzzy evaluation model for urban rivers: A case study in North China. Journal of Water Process Engineering, **67**, 106192, **2024**.
13. LI X., JIANG C., XU Y., GUO P., QUAN C., TONG F., WANG Y. Spatiotemporal correlation of total dissolved solids with karst groundwater levels in the Xiangshan karst region, China. Hydrogeology Journal, **34** (1), 159, **2026**.
14. ALI S.A., ALI U. Hydrochemical Characteristics and Spatial Analysis of Groundwater Quality in Parts of Bundelkhand Massif, India. Applied Water Science, **8**, 39, **2018**.
15. RAJENDRAN R., LAKSHMANAN E., MUDDU S., RAJMOHAN N., VENKATRAMANAN S., BRINDHA K. Multi-indices approach for comprehensive appraisal of groundwater quality and the implication on human health in the Amaravathi basin, Southern India. Environmental Monitoring and Assessment, **197**, 153, **2025**.
16. GRIMA J., LUQUE-ESPINAR J.A., MEJÍA J.A., RODRÍGUEZ R. Methodological approach for the analysis of groundwater quality in the framework of the Groundwater Directive. Environmental Earth Sciences, **74**, 4039, **2015**.
17. YOUNAS F., SARDAR F.M., ULLAH Z., ALI J., YU X., ZHU P., GUO W., AL-ANAZI K.M., FARAH M.A., CUI Z. Assessment of groundwater chemistry to predict arsenic contamination from a canal commanded area: applications of different machine learning models. Environmental Geochemistry and Health, **47** (2), 46, **2025**.
18. SU K., WANG Q., LI L., CAO R., XI Y., LI G. Water quality assessment based on Nemerow pollution index method: A case study of Heilongtan reservoir in central Sichuan province, China. PLoS One, **17** (8), e0273305, **2022**.
19. LI Z., GONG W., YANG H., YU H., CHEN S., GUI H., MIN N., YIN C., XU P. Hydrochemical characteristics and genesis of surface water from subsidence pools in coal mining area of Northern Anhui Province, China. Applied Water Science, **15**, **2025**.
20. ZHANG J., WANG B., LIU T. Fuzzy comprehensive evaluation and its validation for shallow groundwater vulnerability in Jianghan Plain. Bulletin of Geological Science and Technology, **39** (6), 154, **2020** [In Chinese].
21. PANT R.R., AWASTHI M.P., KHANAL B., ACHARYA A., POUDEL P., PARAJULI S., BOHARA R., CHAND M.B., BISHWAKARMA K., THAKUR T.K., KANDEL K. Hydrochemical characteristics and water quality assessment of surface water in the Badigad River Basin, Lesser Himalayas, Nepal. Environmental Science and Pollution Research, **32**, 19836, **2025**.
22. LI H., ZHANG W., WANG Y., Zhang L., LI X., GENG H., LU Y. Chemical characteristics and evolution of groundwater in northeastern margin of the Tibetan Plateau, China. Environmental Geochemistry and Health, **47**, 11, **2025**.
23. ALQARAWY A.M., NATARAJAN R., MASOOD M.H.Z., NIYAZI B.A. Hydrochemical appraisal and sources of contamination in high nitrate aquifer, Saudi Arabia. Arabian Journal of Chemistry, **16** (9), 105041, **2023.**
24. LIU F., ZOU J., LIU J., ZHANG J. ZHEN P. Factors controlling groundwater chemical evolution with the impact of reduced exploitation. Catena, **214** (1),106261, **2022**.
25. DUFERA A.G., LIU T., XU J., WEI Z. Regression models of Pearson correlation coefficient. Statistical Theory and Related Fields, **7**, 97, **2023**.
26. QU J., LIN J., WANG J., YAN T., REN K., ZHOU J. LI Y. Analysis of the evolution and causes of groundwater chemistry after ecological water replenishment of the Jialu River, China. Scientific Reports, **14** (1), 18759, **2024**.
27. JENA M.R., TRIPATHY J.K., SAHOO D., SAHU P. Geochemical Evaluation of Groundwater Quality in the Coastal Aquifers of Kujang Block, Jagatsinghpur District, Eastern Odisha, India. Water, Air, and Soil Pollution, **235**, 349, **2024**.
28. TAWFEEQ J.M.S., DİŞLI E., HAMED M.H. Hydrogeochemical evolution processes, groundwater quality, and non-carcinogenic risk assessment of nitrate-enriched groundwater to human health in different seasons in the Hawler (Erbil) and Bnaslawa Urbans, Iraq. Environmental Science and Pollution Research, **31**, 26182, **2024**.
29. KRISHNAMOORTHY L., LAKSHMANAN V.R. Hydrogeochemical Evaluation and Multivariate Statistical Analysis of Groundwater for Sustainable Groundwater Quality Management in the Industrial Corridor of Ranipet District, Tamil Nadu, India. Water, Air, & Soil Pollution, **235**, 644, **2024**.
30. LIU N., CHEN M., GAO D., WU Y., WANG X. Identification of hydrogeochemical processes in shallow groundwater using multivariate statistical analysis and inverse geochemical modeling. Environmental Monitoring and Assessment, **197**, 135, **2025**.
31. AHMAD A.B. Assessing Sirwan River Water Quality based on a single-factor assessment and comprehensive pollution index methods. Journal of Kirkuk University for Agricultural Sciences, **14** (4), 153, **2023**.
32. M. Al-SULAIMAN A., S. RUSOL M.M., AL-OBAIDI BASIM H.K. Water Quality Evaluation of Diwaniyah River Using The Nemerow Pollution Index. Kufa Journal of Engineering, **16** (2), 1, **2025**.